APPENDIX E

RADAR SIMULATION

INTRODUCTION

This appendix discusses the techniques used to simulate the primary radar performance so that trade-off investigations could be made as a function of radar signal processing characteristics in the presence of a parametric range of noise, desired signal, and asynchronous interfering signal conditions. The primary radar simulated was the ASR-7. Only the normal and Moving Target Indicator (MTI) channels of the radar were simulated. The portion of the ASR-7 radar simulated was the processor unit (i.e., normal channel envelope detector output and MTI channel phase detector output to the radar output).

In addition, for study of the properties of the feedback enhancer, the simulation provides the capability to use a feedback enhancer in place of the ASR-7 binary enhancer. It should be noted however, that the ASR-7 does not have a feedback enhancer.

PROCESSOR UNIT DESCRIPTION

A detailed description of the primary radar processor unit is given in Section 3. Figure E-1 shows a block diagram of the ASR-7 processor unit hardware which was simulated. The portion of the processor unit normal channel simulated was the normal channel enhancer functional switch, enhancer and alignment hardware. The portion of the processor unit MTI channel simulated was the MTI cancellers, enhancer functional switch, enhancer, and alignment hardware. The simulation model has the capability of displaying the processor unit output in the unenhanced and enhanced modes of both the normal and MTI channels on either an oscilloscope or Plan Position Indicator (PPI) display.

In order to reduce the simulation model computer run time and for analytical simplicity, the conventional analog-to-digital (A/D) and digital-to-analog (D/A) converters at the processor unit input and output respectively were not simulated. However, the received signal amplitudes were simulated in time by dividing the radar receive period after each transmitted pulse into 1200 range bins .625 microseconds long corresponding to the actual A/D and D/A converter hardware of the ASR-7. Since the quantization noise caused by A/D converters is small compared to the inherent receiver noise, not simulating the A/D and D/A converters will not result in unrealistic simulation of the ASR-7 processor unit.

The clock timing for the range bins and desired signal characteristics are shown in Figure E-2. The ASR-7 system clock timing and desired signal

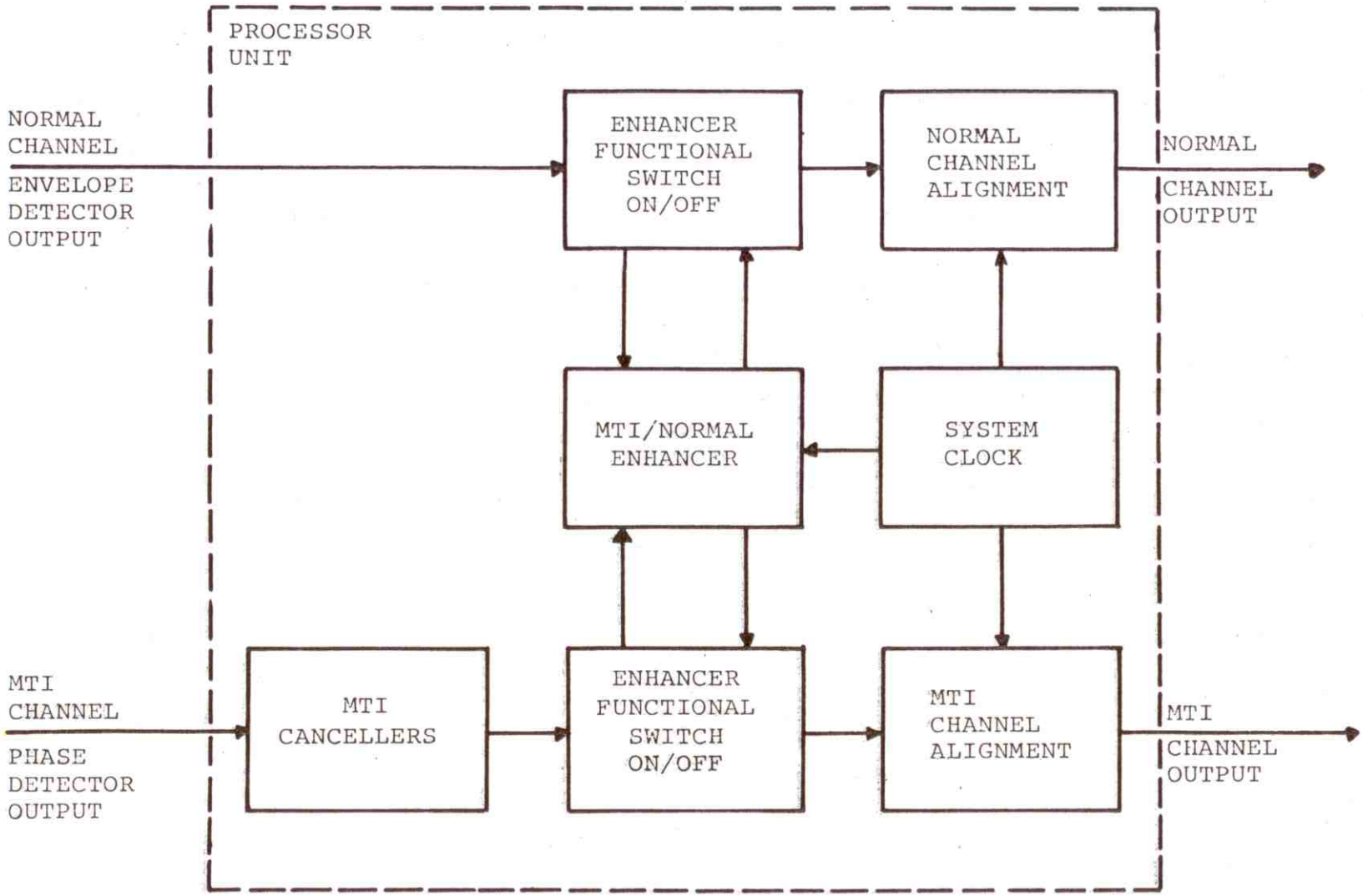

Figure E-1. Block Diagram of Simulated ASR-7 Processor Unit

PW = 0.833 μsec

PRF = 1002 Average (6-Pulse Stagger)

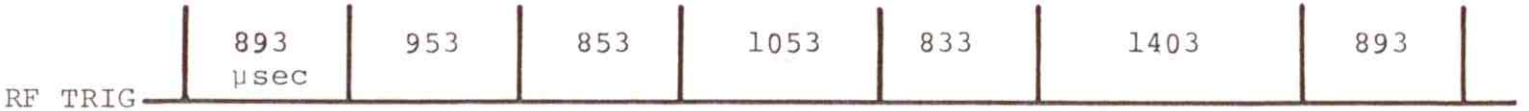

Figure E-2. Clock Timing and Desired Signal Characteristics for ASR-7 Radar

characteristics were simulated for the radar operating in the six-stagger mode which has an average Pulse-Repetition-Frequency (PRF) of 1002 Pulses-Per-Second (PPS). The clock timing also controls the video realignment (destaggering to an average PRF of 1002) at the processor output for Plan Position Indicator (PPI) display. Using the nominal ASR-7 characteristics, the degrees of antenna scan per pulse (ϕ_S) is given by:

$$\phi_S = \frac{6 \cdot RPM}{PRF} = \frac{6 \cdot 12}{1002} = 0.0718562874°/pulse \qquad \text{(E-1)}$$

where:

RPM = Antenna scan rate, in rpm (12 for ASR-7)

PRF = Radar pulse repetition frequency, in PPS (1002 for ASR-7)

The number of Azimuth Change Pulses (ACP) per antenna scan for the ASR-7 is:

$$ACP = \frac{360°}{\phi_S} = 5010 \qquad \text{(E-2)}$$

Therefore, in summary the simulation of the ASR-7 processor unit was done by:

a. Dividing the receive period after each pulse into 1200 range bins .625 microseconds long,

b. each range bin is approximately 0.0718 degrees wide, and

c. there are 5010 azimuth change pulses (ACPs) per antenna scan.

DESIRED SIGNAL

Figure E-2 shows the pulse width and PRF stagger sequence of the ASR-7 desired signal. The radar simulation model has the capability of simulating a single desired target at any specified range and bearing. The received desired signal pulse train (number of pulses from a target (N)) consists of 20 pulses determined by:

$$N = \frac{PRF \cdot BW}{6 \cdot RPM} = \frac{(1002)(1.5)}{(6)(12)} \simeq 20 \qquad \text{(E-3)}$$

where:

PRF = Radar pulse repetition frequency, in PPS (1002 for ASR-7)

BW = Antenna 3 dB beamwidth, in degrees (1.5 degrees for ASR-7)

RPM = Antenna scan rate, in rpm (12 for ASR-7)

The range bin in which the target is located (TRB) was calculated by:

$$TRB = \frac{TR}{RTT \cdot RBT} \qquad \text{(E-4)}$$

where:

TRB = Target range bin location, between 1 and 1200

TR = Target range, in nautical miles

RTT = Round-trip time, equals .081 nautical miles per microsecond

RBT = Range bin time, equals .625 microseconds per range bin

The target location (bearing) in Azimuth Change Pulses (ACP) was calculated by:

$$TACP = \frac{TB \cdot PRF}{6 \cdot RPM} \qquad \text{(E-5)}$$

where:

TACP = Target azimuth change pulse, between 1 and 5010

TB = Target bearing, in degrees

PRF = Radar pulse repetition frequency, in PPS (1002 for ASR-7)

RPM = Antenna scan rate, in rpm (12 for ASR-7)

The desired signal voltage amplitude in each range bin as a function of the desired signal signal-to-noise ratio (S/N) is discussed later in the normal and MTI channel simulation sections.

INTERFERING SIGNALS

Three types of interfering radar signals were simulated: ASR-5, ASR-8, and AN/FPS-90. The radar simulation model has the capability of having any combination of the three interfering sources present. Figures E-3 through E-5 show the signal timing characteristics of the ASR-5, ASR-8, and AN/FPS-90 interfering radars used in the simulation model. The interfering signal voltage amplitude in each range bin as a function of the interference-to-noise ratio (I/N) is discussed later in the normal and MTI channel simulation sections.

NOISE

In range bins where there was no desired signal or interfering signal the radar inherent noise level was simulated. The simulation of the noise amplitude in each range bin is discussed in the normal and MTI channel simulation sections.

NORMAL CHANNEL SIMULATION

The following is a discussion of the techniques used to simulate the noise, desired signal, and interfering signal levels in the normal channel, and the processor unit hardware in the normal channel.

Noise Distribution

The voltage amplitude distribution of the noise at the normal channel envelope detector output is Rayleigh distributed. The Rayleigh distributed voltage amplitude characteristics of the noise were simulated by letting

$$n_{edo}(t) = \sigma\sqrt{-2 \ln U} \qquad \text{(E-6)}$$

where:

σ = RMS noise level at detector input, in volts

U = Random number uniformly distributed between 0 and 1.0

For each range bin in which noise only is present, a noise voltage amplitude using Equation E-6 was simulated by randomly selecting values between 0 and 1.0 for U.

Signal-Plus-Noise Distribution

The signal-plus-noise voltage amplitude distribution at the envelope detector output has a Rice distribution (also called the Marcum "Q" function). The amplitude characteristics of the signal-plus-noise for the

PW = 0.833 μsec
PRF = 1170 Average (2-Pulse Stagger)

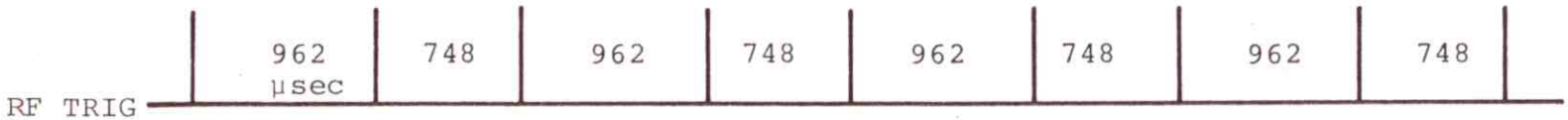

Figure E-3. ASR-5 Interfering Signal Characteristics

PW = 0.6 μsec
PRF = 1040 Average (4-Pulse Stagger)

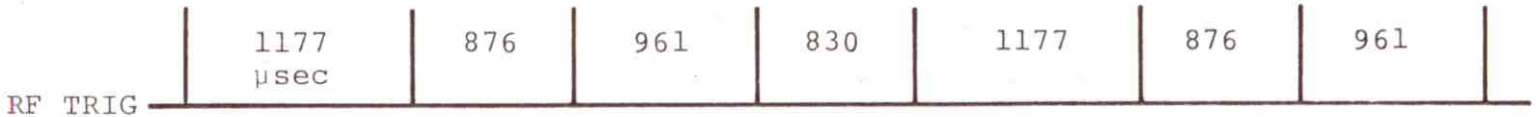

Figure E-4. ASR-8 Interfering Signal Characteristics

PW = 2.0 μsec
PRF = 370 Pulses

Figure E-5. AN/FPS-90 Interfering Signal Characteristics

desired and interfering signals were simulated by:

$$(S+N)_{edo}(t) = \sqrt{X^2+Y^2} \qquad \text{(E-7)}$$

where:

$X = R \cos(2\pi V) + A$

$Y = R \sin(2\pi V)$

$R = \sigma\sqrt{-2 \ln U}$

σ = RMS noise level at envelope detector input, in volts

A = Peak-signal level at envelope detector input, in volts

U and V = Random numbers between 0 and 1.0

For the case where "A" equals zero (no signal present), Equation E-7 is equivalent to Equation E-6. Equation E-7 was used to simulate the signal-plus-noise voltage amplitude for both the desired pulse train and interfering signal. The timing of the desired and undesired signals were programmed using List Processing Techniques. For each range bin in which a desired or interfering pulse is present, a signal-plus-noise voltage amplitude using Equation E-7 was simulated by randomly selecting values between 0 and 1.0 for U and V. Figure E-6 shows the simulated signal-plus-noise voltage amplitude distribution as a function of the signal-to-noise ratio (S/N) in dB generated using Equation E-7. The RMS noise voltage level (σ) was set at .25 volts. This corresponds to a one volt peak noise level generally set at the radar receiver output.

Normal Channel Enhancer

The ASR-7 enhancer hardware which was simulated is shown in Figure E-7. The enhancer is basically a digital circuit with an adjustable threshold detector as a simple A/D converter. The enhancer circuit consists of the threshold detector, the digital adder/subtracter circuits, a full range shift register storage, and a D/A converter. If an echo signal exceeding the set threshold level exists in any given range bin, the enhancer stores a one level digital signal in its shift register memory. If the signal continues above the threshold in the given range bin, the enhancer will increase the level stored in each PRF period until a maximum amplitude of 31 is reached. If in any PRF period the signal fails to exceed the threshold level, the enhancer subtracts from the stored level in that particular range bin. The clock timing for the shift register was simulated for the ASR-7 six-stagger mode (see Figure E-2).

A detailed discussion of the signal processing properties of the ASR-7 enhancer is given in Appendix D.

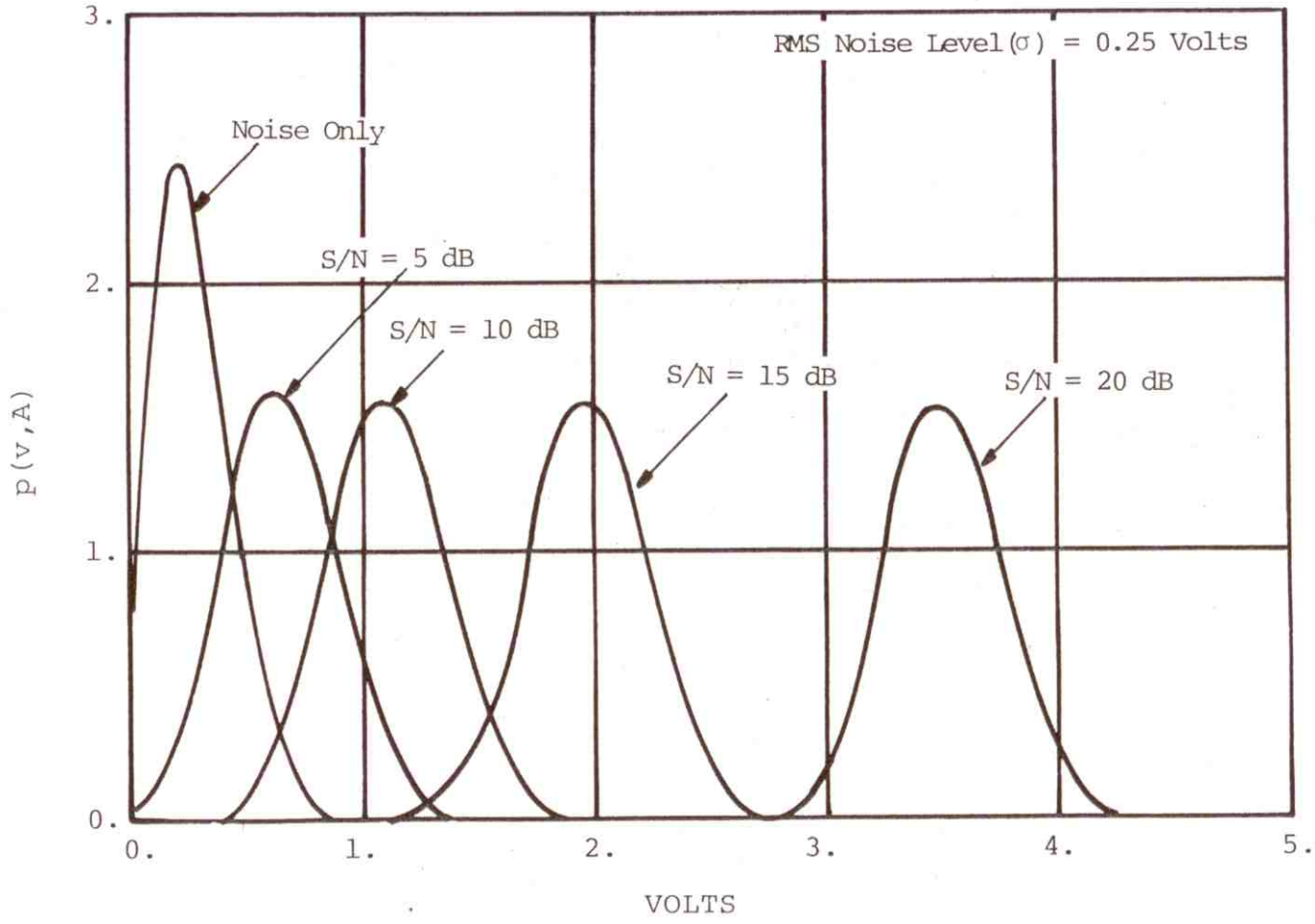

Figure E-6. Probability Density Function for Noise Only and for Signal-Plus-Noise at the Normal Channel Envelope Detector Output.

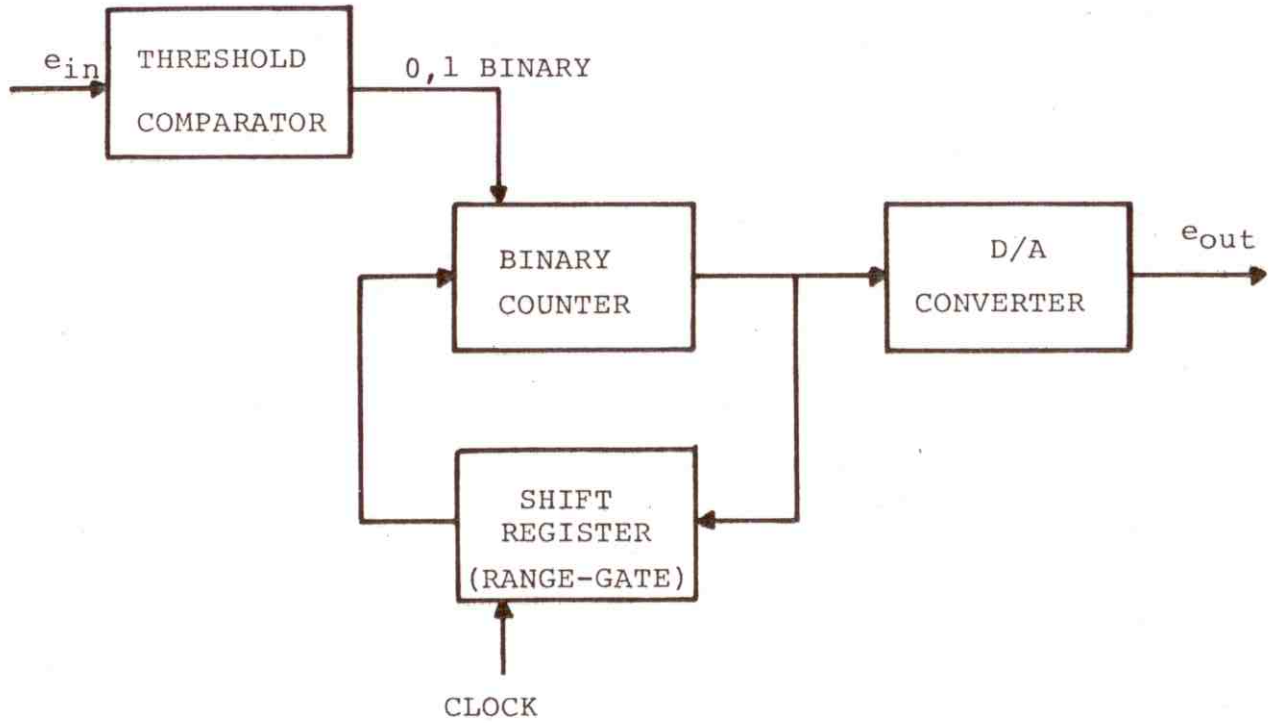

Figure E-7. ASR-7 (AN/GPN-12) Binary Integrator Block Diagram

Normal Channel Alignment

The normal channel alignment circuits provide the delay required during STAGGER PRF operation to insure that a specific range bin in each PRF receive period occurs at the average PRF of 1002. The STAGGER PRF operation and clock timing which was simulated is shown in Figure E-2. The stagger video occurs with the PRF periods of 893 microseconds, 953 microseconds, 853 microseconds, 1053 microseconds, 833 microseconds, and 1403 microseconds. To align these with the average period of 998 microseconds, clock timing from the RF trigger is used to control the alignment circuit delay selection.

MTI CHANNEL SIMULATION

The following is a discussion of the techniques used to simulate the noise, desired signal, and interfering signal in the MTI channel, and the processor unit hardware in the MTI channel.

Noise Distribution

The voltage amplitude distribution of the noise at the phase detector output is Gaussian distributed. The Gaussian distributed voltage amplitude characteristics of the noise were simulated by letting:

$$n_{pdo}(t) = R \cos 2\pi V \qquad \text{(E-8)}$$

where:

$R = \sigma\sqrt{-2 \ln U}$

σ = RMS noise level at phase detector input, in volts

U and V = Random numbers uniformly distributed between 0 and 1.0

For each range bin in which noise only is present, a noise voltage amplitude using Equation E-8 was simulated by randomly selecting values between 0 and 1.0 for U and V.

Signal-Plus-Noise Distribution

The signal-plus-noise voltage amplitude distribution at the phase detector output was simulated by:

$$(S+N)_{pdo}(t) = R \text{ Cos } 2\pi V + A \cos 2\pi W \qquad \text{(E-9)}$$

where:

A = Peak-signal level at phase detector input, in volts

V and W = Random numbers uniformly distributed between 0 and 1.0

For the case where "A" equals zero (no signal present), Equation E-9 is equivalent to Equation E-8. Equation E-9 was used to simulate the signal-plus-noise voltage amplitude for both the desired pulse train and interfering signal. The timing of the desired and undesired signals were programmed using List Processing Techniques. For each range bin in which a desired or interfering pulse is present, a signal-plus-noise voltage amplitude using Equation E-9 was simulated by randomly selecting values between 0 and 1.0 for U, V, and W. Figure E-8 shows the simulated signal-plus-noise voltage amplitude distribution as a function of the signal-to-noise ratio (S/N) in dB generated using Equation E-9. The rms noise voltage level was set at .25 volts.

MTI Cancellers

The MTI double stage canceller hardware in the ASR-7 radar was simulated. It was necessary to simulate the ASR-7 MTI canceller hardware in order to investigate the performance of the ASR-7 enhancer in the presence of asynchronous interference since the impulse response of a double stage MTI canceller with feedback will produce several synchronous pulses. A detailed discussion of the signal transfer properties of a double stage MTI canceller to asynchronous interference is discussed in Appendix C. The following is a discussion of the simulation of the ASR-7 double stage MTI canceller.

The ASR-7 digital canceller consists of two identical delay line type cancellers in cascade, with switch selectable feedback. Figure E-9 shows the canonical form of the ASR-7 MTI canceller which was simulated. The figure shows the transfer function coefficients which represent the ASR-7 hardware. The feedforward coefficients (a_i) are $a_o = 1/2$, $a_1 = -1$, and $a_2 = 1/2$. The feedback coefficients (b_i) for the various canceller modes are:

CANC 2 :	$b_1 = 0$;	$b_2 = 0$
25 dB SCV:	$b_1 = 1\frac{1}{4}$;	$b_2 = -\frac{1}{2}$
30 dB SCV:	$b_1 = 1$;	$b_2 = -\frac{1}{2}$
35 dB SCV:	$b_1 = \frac{3}{4}$;	$b_2 = -\frac{1}{2}$
40 dB SCV:	$b_1 = \frac{1}{2}$;	$b_2 = -\frac{1}{2}$

A digital word from each range bin is fed into the canceller. If this range bin contains only clutter, the canceller output will be virtually zero. If it contains a moving target the difference amplitude will represent a sample taken from the doppler cycle. The storage element in each canceller consists of eight parallel shift register chains 1200 range bins long. The digital words are clocked in parallel down the 1200 shift-register bins at a 1.6 MHz rate. The timing for the delays in the MTI canceller were simulated for the ASR-7 six-stagger mode shown in Figure E-2. List Processing Techniques were

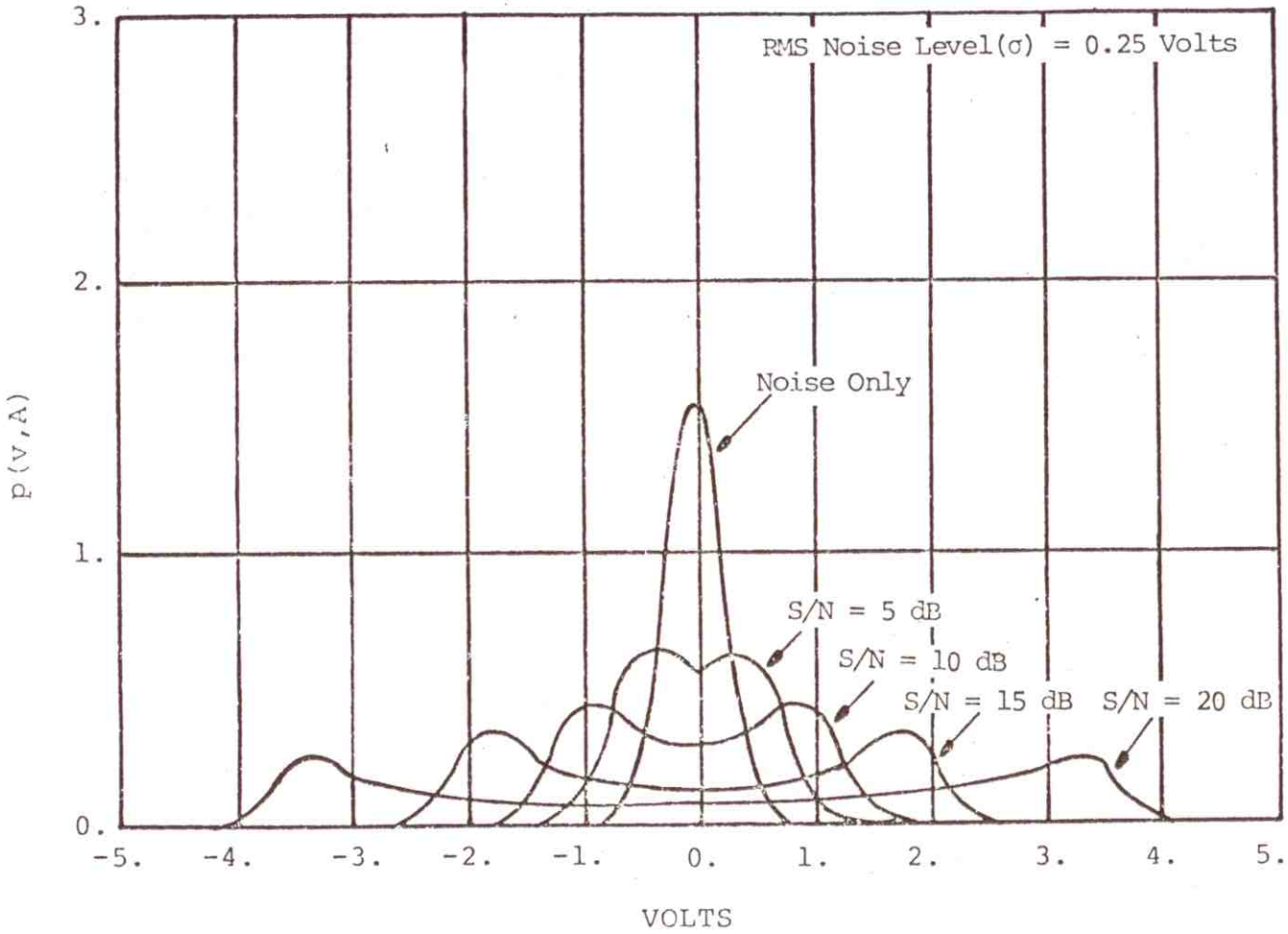

Figure E-8. Probability Density Function for Noise Only and for Signal-Plus-Noise at the MTI Phase Detector Output.

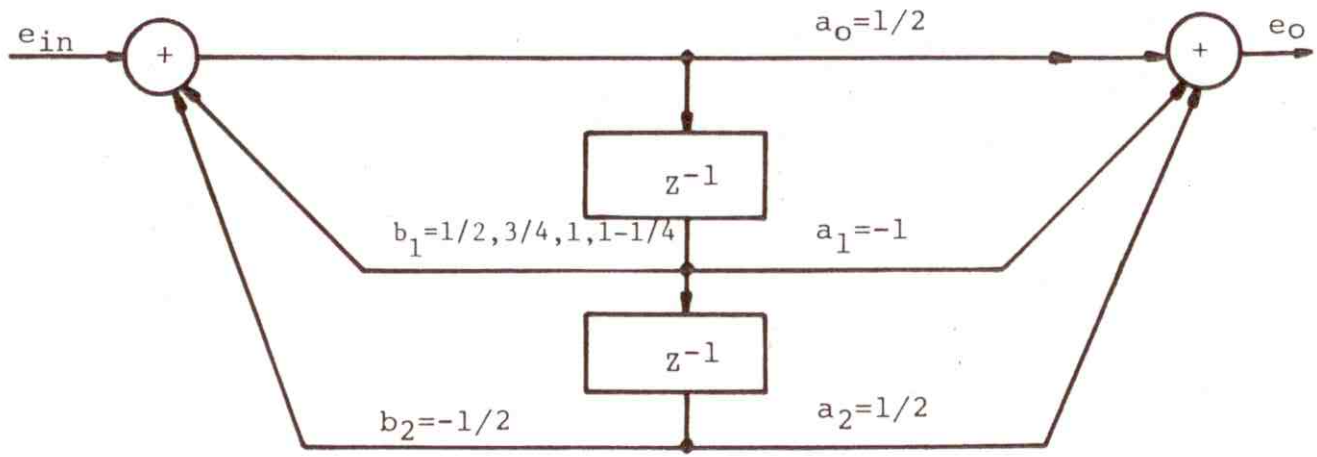

Figure E-9. Canonical Form of Simulated ASR-7 MTI Canceller

used in programming the timing of the ASR-7 six-stagger sequence.

Appendix C contains a detailed discussion of the signal processing properties of the MTI cancellers.

MTI Channel Enhancer

The MTI channel enhancer circuitry is identical to the normal channel enhancer. The simulation of the enhancer was discussed in the normal channel simulation section.

MTI Channel Alignment

The MTI channel alignment circuitry is identical to the normal channel alignment circuitry. The simulation of the alignment circuitry was discussed in the normal channel simulation section.

FEEDBACK ENHANCER

As mentioned at the beginning of this appendix, a feedback enhancer capability was added to the simulation. Figure E-10 shows the feedback enhancer model used in the simulation. The first three blocks: the attenuator, subtractor and bottom clipper are ,strictly speaking, not part of the ASR-8 enhancer circuit board (which it attempts to model). However, these functions are effectively found in other circuits, and it was found necessary to include them to achieve realistic results. Appendix D has a detailed discussion of the feedback integrator.

OUTPUT DISPLAY

Two radar output displays were simulated: the radar output oscilloscope display, and the radar output PPI display. The radar simulation model has the capability of displaying both the normal and MTI channels in the unenhanced and enhanced modes. Appendix D contains oscilloscope display outputs as a function of a parametric range of noise, desired signal, and asynchronous interfering conditions. Also, the trade-offs of the desired signal properties in utilizing an enhancer to suppress interfering signals are discussed in Appendix D. Figure E-11 is 45 degrees of a simulated PPI display of interference.

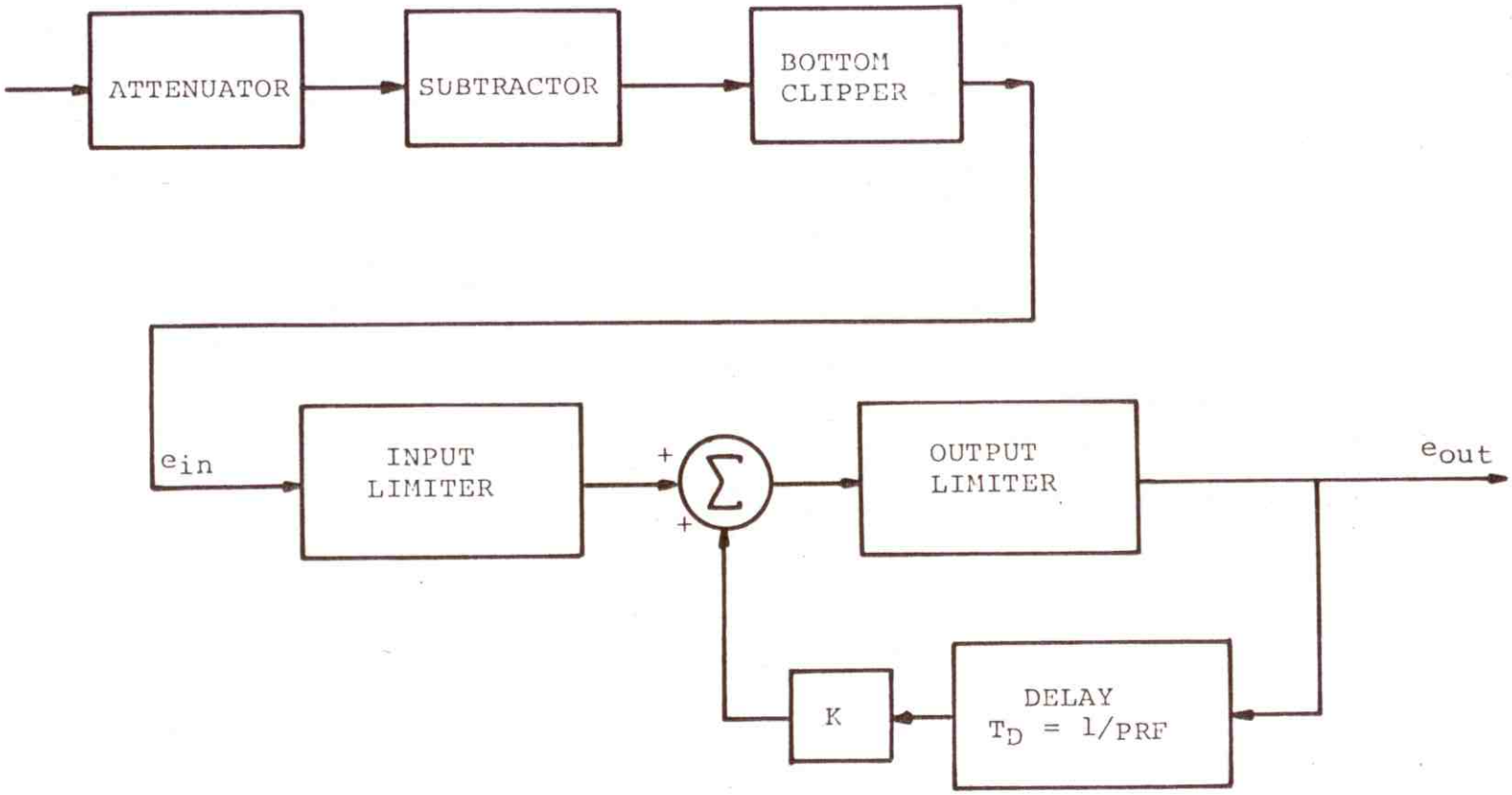

Figure E-10. Feedback Integrator Block Diagram

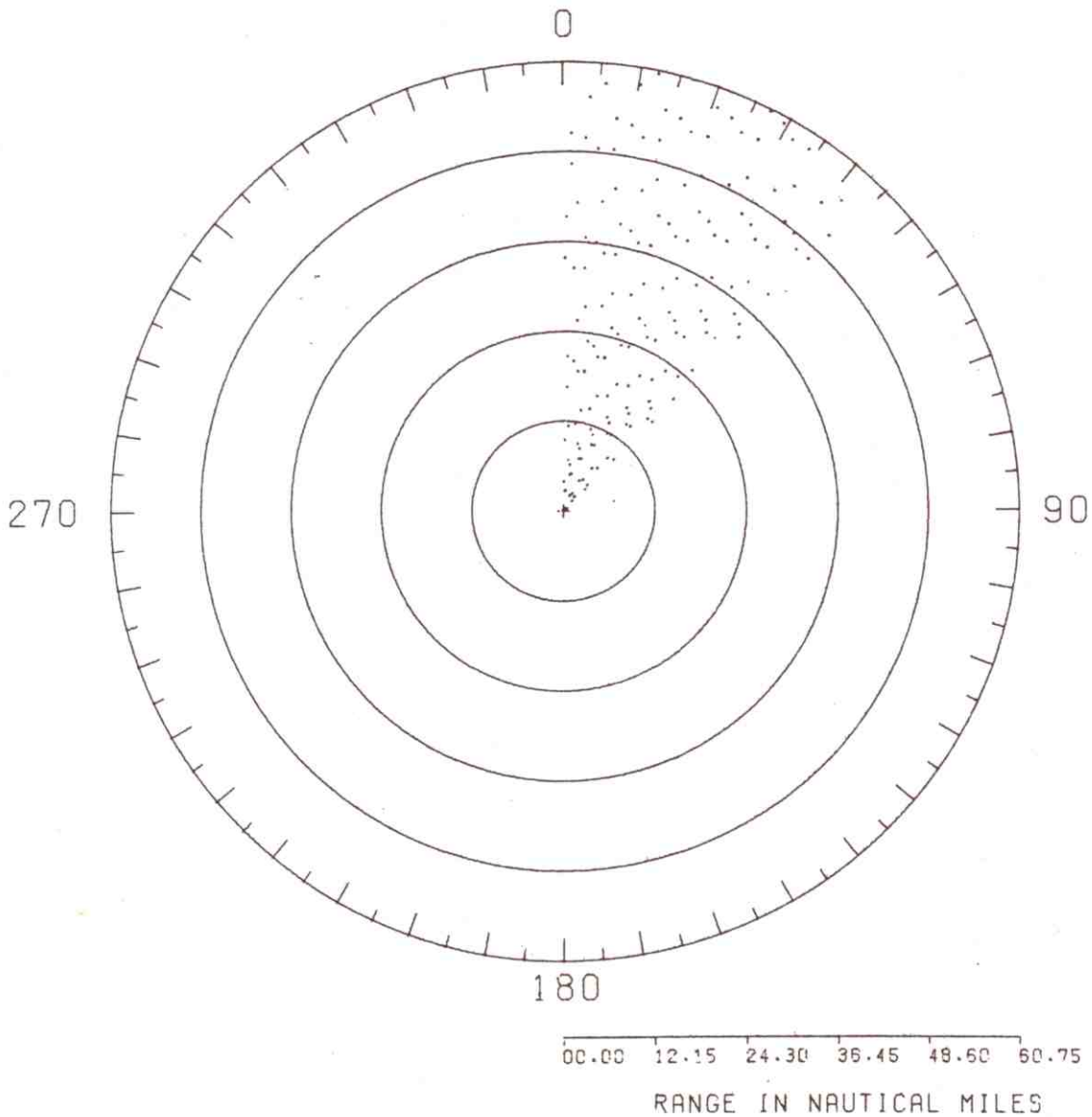

Figure E-11. Simulated PPI Display of Interference

APPENDIX F

INTRODUCTION

This Appendix includes derivations of the equations, and a description of the computer programs used to analyze the impact of radar pulse interference on ARTS-IIIA/RDAS performance. The first section derives the equation used to evaluate the effect of interference on target and false target hit probabilites. The derivation of equations used to compute clutter hit, target hit, and noise hit probability are also included in the first section. The second section describes computer programs that were written to compute the probability of false alarm and target detection.

DERIVATION OF EQUATIONS

Effect of Interference on Hit Probability

The following is a derivation of the equation that gives the probability of a hit (logical 1) at the rank order detection process (includes the rank quantizer and hit processor shown in Figure 4-4) output when interference is present. The derived equation is a general equation that can be used to determine the effect of interference on the probability of a hit (logical 1) when noise, desired signal or clutter are in the range bin of interest. The effect of interference on the probability of a hit when noise, desired signal, or clutter is present in the range bin of interest is a function of the probability of a hit (logical 1) when noise only is present (P_{nl}), probability of a hit when noise and desired signal only are present (P_{sl}), and the probability of a hit when noise and clutter only are present (P_{cl}), respectively. For purposes of deriving a general equation for all of the above conditions, a general term (P_1) will be used to represent a hit for P_{nl}, P_{sl}, and P_{cl}. The equations for P_{nl}, P_{sl}, and P_{cl} will then be derived later. The derivations are described for a rank quantizer threshold 24 to minimize verbiage. However, the results are applicable to any rank quantizer threshold.

The rank order detection processing technique employed in the Radar Data Acquisition Subsystem (RDAS) involves comparing the voltage level in the range bin of interest with that in 24 other adjacent range bins. A logical 1 or hit is generated if the voltage level in the range bin of interest exceeds a particular number (rank quantizer threshold) of the adjacent comparison range bins. If it is assumed that no interfering pulses fall in the comparison range bins and, the level of the interfering pulses is always greater than the voltage level in the comparison range bins, a hit will be generated every time an interference pulse falls in the range bin of interest. Let A represent the event in which one or more interfering pulses fall in the range bin of interest. A hit can also be generated without the presence of interference if the voltage level due to signal-plus-noise, noise only, or clutter exceeds the voltage level in the comparison range bins. Let B represent the event in which a hit is generated when no interference is

present. The probability of a hit being generated with interference or without interference is given by (Davenport, 1958):

$$P(A \cup B) = P(A) + P(B) - P(A \cap B) \qquad \text{(F-1)}$$

where A U B represents the event in which A or B occurs and A ∩ B represents the event in which both A and B occur. Since events A and B are independent of each other, Equation F-1 can be written in the form:

$$P(A \cup B) = P(A) + P(B) - P(A)P(B) \qquad \text{(F-2)}$$

The generation of a hit (logical 1) can be inhibited if a strong interfering pulse falls in one or more of the rank quantizer comparison range bins, because the voltage level in the range bin of interest will then not exceed all the comparison range bin voltage levels. The following derivations assume that all the interfering pulses are the same level, and as previously stated, greater than the noise, clutter, or target voltage level. These assumptions imply that an interfering pulse falling in the rank quantizer range bin of interest will not generate a hit if one or more of the interfering pulses simultaneously fall into the rank quantizer comparison range bins. Let C represent the event of an interfering pulse falling into one or more of the comparison range bins, and P(C) the probability of that event occurring. A hit can only occur if event A or B occurs and no interfering pulses fall in the comparison range bins. Since Equation F-2 gives the probability of A or B occurring and 1-P(C) the probability of an interfering pulse not falling in the comparison range bins, the probability of a hit occurring with interference present is given by:

$$P_{il} = [P(A) + P(B) - P(A)P(B)][1-P(C)] \qquad \text{(F-3)}$$

The product of Equation F-2 and [1-P(C)] is used in Equation F-3 because event C can be considered independent of events A and B. This is possible because the interfering pulses arrive randomly in time and the no interference voltage level is assumed to be insignificant compared with the level of the interfering pulses.

Equation F-3 defines the probability of a hit due to asynchronous interference for the ARTS-IIIA/RDAS connected to the victim radar normal channel. This equation will be expanded for the case in which the ARTS-IIIA/RDAS is connected to the radar MTI channel. Approximately three synchronous interfering pulses are generated by the MTI canceller circuits for each asynchronous interference pulse at its input. This affects the probability of interfering pulses falling in a given rank quantizer range bin. An interfering pulse falling in the rank quantizer range bin of

interest could be due to an asynchronous interfering pulse at the input of the MTI falling in the range bin of interest on the present ACP (event A_1), previous ACP (event A_2), or two ACPs before (event A_3). Therefore, the probability of an interfering pulse falling in the rank quantizer range bin of interest is given by:

$$P(A_1 U A_2 U A_3) = P(A_1)+P(A_2)+P(A_3) - P(A_1 \cap A_2) - P(A_1 \cap A_3) - P(A_2 \cap A_3) + P(A_1 \cap A_2 \cap A_3) \qquad \text{(F-4)}$$

Since the probability of an asynchronous interfering pulse falling in a particular range bin is the same for all ACPs, and independent of each other, Equation F-4 can be written in the form:

$$P(A_1 U A_2 U A_3) = 3P(A) - 3[P(A)]^2 + [P(A)]^3 \qquad \text{(F-5)}$$

Equation F-5 can be closely approximated by $3P(A)$ since $P(A)<10^{-4}$ and the product terms are small compared to $3P(A)$.

Based on the assumptions in this analysis, it is required that no interfering pulses fall in the rank quantizer comparison range bins for a hit to be generated. In order for this to occur with the ARTS-IIIA/RDAS connected to the MTI channel, it is necessary that interfering pulses do not fall in these range bins at the MTI circuit input for three consecutive ACPs. It was previously shown that $1-P(C)$ is the probability of an interfering pulse not falling in the comparison range bins, where $P(C)$ is the probability of interfering pulses falling in the comparison range bins. Therefore, the probability of interfering pulses not falling in the comparison range bin for three consecutive ACPs is $[1-P(C)]^3$. Substituting $[1-P(C)]^3$ for $[1-P(C)]$ and $3P(A)$ for $P(A)$ in Equation F-3 gives:

$$P_{il} = [3P(A) + P(B) - 3P(A)P(B)]\ [1-P(C)]^3 \qquad \text{(F-6)}$$

Equations F-3 and F-6 can be represented by one general equation

$$P_{il} = [N\,P(A) + P(B) - N\,P(A)\,P(B)]\ [1-P(C)]^N \qquad \text{(F-7)}$$

where N is set equal to 1 for the ARTS-IIIA/RDAS connected to the radar normal channel and set equal to 3 if connected to the MTI channel.

The random arrival of asynchronous interfering pulses in time can be described by a Poisson probability distribution (Davenport, 1958).

Therefore, the probability of an interfering pulse overlapping the sample time of the range bin of interest is given by:

$$P(A) = 1-e^{-x_1\nu} \qquad \text{(F-8)}$$

where:

X_1 = Time interval that an interfering radar pulse can overlap the sample time of the rank quantizer range bin of interest, seconds

ν = Interfering pulse arrival rate, pulses/second

The probability of an interfering pulse overlapping the sample time of one or more comparison range bins is given by:

$$P(C) = 1-e^{-x_2\nu} \qquad \text{(F-9)}$$

where:

X_2 = Time interval that an interfering radar pulse can overlap one or more of the rank quantizer comparison range bins sample times, seconds

Substituting Equations F-8 and F-9 into Equation F-7 and letting the probability of a hit without interference, P(B), equal P_1 gives:

$$P_{il} = [N(1-e^{-x_1\nu})+P_1-N(1-e^{-x_1\nu})P_1][1-(1-e^{-x_2\nu})]^N \qquad \text{(F-10)}$$

Algebraic simplification of this equation gives the basic equation that was used in the analysis:

$$P_{il} = [N(1-P_1)(1-e^{-x_1\nu}) + P_1]e^{-Nx_2\nu} \qquad \text{(F-11)}$$

Some justification for the assumption that the interfering pulses are greater than the target return pulses at the ASR-7 radar MTI circuit output needs to be presented, since the amplitude of a given interfering pulse out of the ASR-7 MTI circuit can be zero depending on its phase angle relative to the COHO reference signal. For example, the MTI phase detection in the ASR-7 radar will give a zero output voltage if the difference in phase between the interfering pulse and the coherent oscillator signal is 90 degrees (see Appendix C). The simulation of interfering radar effects on the ASR-7 radar

(see Appendix E) involved obtaining pulse amplitude statistics at the MTI circuit output. A modified cumulative distribution of these statistics are shown in Figure F-1 for various signal-to-noise ratios (SNR's). The vertical axis gives the percentage of time that the horizontal axis signal-plus-noise voltage level is exceeded. The curves are applicable to either randomly arriving constant amplitude interfering or target return pulses since the simulations assumed no phase correlation between pulses. The curves in Figure F-1 indicate that if the interfering pulse levels are much greater than the target return pulses at the input of the MTI circuits, there is a high probability that this condition will also exist at the MTI circuit outputs (ARTS-IIIA/RDAS input). For example, assume that the interference-to-noise ratio (INR=20 dB) is 10 dB greater than the signal-to-noise ratio (SNR=10 dB). For this case, Figure F-1 indicates the interference-plus-noise level would exceed 1.5 volts at the MTI output 60 percent of the time while the signal-plus-noise level would exceed this level only 2 percent of the time. This example indicates that it is reasonable to make the worst-case assumption that the interfering pulses are greater than the target return pulses at the ARTS-IIIA/RDAS input when connected to the ASR-7 MTI channel. This worst-case assumption is even more reasonable for the ASR-8 radar dual channel MTI since it employs quadrature phase detectors. A single non-zero amplitude pulse at the dual channel MTI input, regardless of its phase, will not be zero amplitude at its output.

Probability of False Target Hit

This subsection derives the equation for probability of a false target hit due to noise without the presence of interference. A false target hit is defined as the generation of a target hit (logical 1) when no target is present. A hit is generated for these conditions if the noise level in the rank quantizer range bin of interest is greater than RQT of the J comparison range bins. This rank order detection process results in a constant false target hit probability if the rank quantizer range bin sample outputs V_1, V_2, ..., V_j, V_{j+1} are independent and identically distributed. These statistical conditions are assumed for the following derivations. Let F define the cumulative distribution,

$F(v) = P(V<v)$, where V represents rank quantizer comparison range bin samples. In J independent noise samples V_i, i=1,....J, from the J rank quantizer comparison range bins, the probability that exactly RQT (rank quantizer threshold) will be less than the J+1 sample (sample from rank quantizer range bin of interest) is given by:

$$\binom{J}{RQT} [F(v)]^{RQT} [1-F(v)]^{J-RQT} \qquad \text{(F-12)}$$

The value of v in this equation represents the noise voltage level in the range bin of interest. The binomial coefficient in Equation F-12 takes into

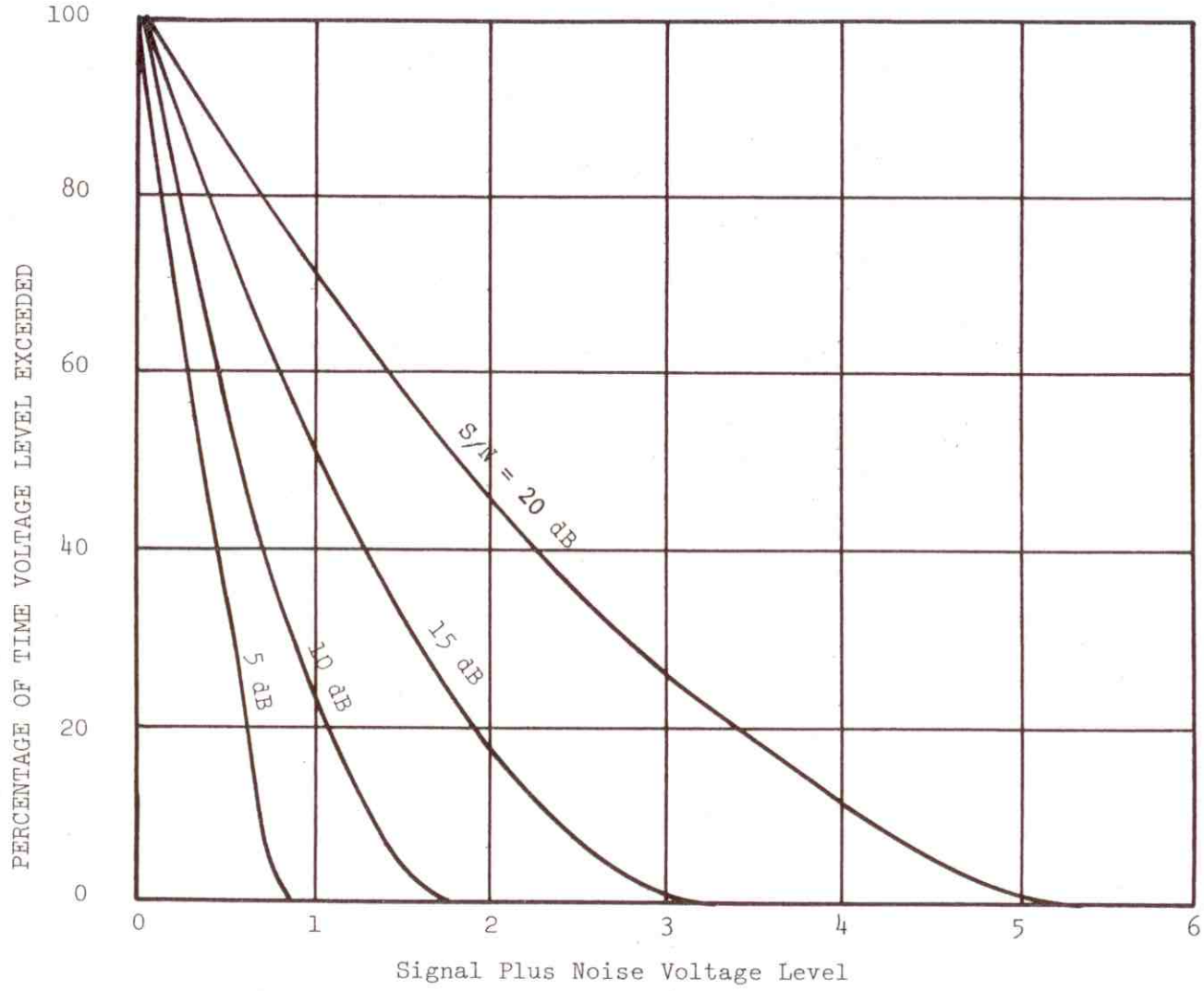

Figure F-1. Modified Cumulative Distribution of Signal-Plus-Noise at ASR-7 Radar MTI Channel Output for Various Signal-to-Noise Voltage Ratios

account the different combinations of RQT out of J things. The probability that the sample in the rank quantizer range bin of interest is greater than RQT of J comparison range bins is given by:

$$\sum_{K=RQT}^{J} \binom{J}{K} [F(v)]^K [1-F(v)]^{J-K} \qquad \text{(F-13)}$$

The value v can be considered sample values drawn from the rank quantizer range bin of interest. If it is assumed that this sample space has a cumulative distribution F(v), taking the expected value of the Equation F-13 gives the probability (P_{n1}) that a sample from the rank quantizer range bin of interest will exceed RQT of the rank quantizer comparison range bin sample levels:

$$P_{n1} = \int_o^1 \sum_{K=RQT} \binom{J}{K} [F(v)]^K [1-F(v)]^{J-K} d[F(v)]$$

$$= \sum_{K=RQT}^{J} \int_o^1 \binom{J}{K} [F(v)]^K [1-F(v)]^{J-K} d[F(v)] \qquad \text{(F-14)}$$

This equation gives the probability of a false target hit occurring due to only noise. A general term in Equation F-14 is:

$$\int_o^1 \binom{J}{K} [F(v)]^K [1-F(v)]^{J-K} d[F(v)] \qquad \text{(F-15)}$$

Substituting the dummy variable u for F(v) and evaluation of F-15 by repeated integration by parts gives:

$$\int_o^1 \binom{J}{K} u^K (1-u)^{J-K} du = \frac{1}{J+1} \qquad \text{(F-16)}$$

Substituting Equation F-16 for each term in Equation F-14 gives:

$$P_{n1} = \sum_{K=RQT}^{J} \frac{1}{J+1} = \frac{J+1-RQT}{J+1} \qquad \text{(F-17)}$$

This equation indicates that the probability of a false target hit due to noise is independent of the noise distribution F(v) and only a function of hardware parameters. It should, however, be reiterated that the equation is only valid when range bin noise samples are independent and identically distributed. The equation would only give approximate false hit values for correlated clutter.

Probability of Target Hit

This subsection derives the equation for probability of target hit without interference present. A target hit is defined as the generation of a target hit (logical 1) when a target is present. The derivation considers the target signal present in the rank quantizer range bin of interest and no target signal present in the rank quantizer comparison range bins. Assume that the samples from the comparison range bins are independent and identically distributed with a cumulative distribution function $F(v) = P(V<v)$. The probability of the target signal-plus-noise level in the range bin of interest being greater than the level in RQT of the J comparison range bins is therefore given by:

$$\sum_{K=RQT}^{J} \binom{J}{K} [F(v)]^K [1-F(v)]^{J-K} \qquad \text{(F-18)}$$

The value v in this equation represents the signal-plus-noise voltage level in the range bin of interest. Assume that the target-plus-noise-signal level v in the rank quantizer range bin of interest has a cumulative distribution function $G(v) = P_{s+n}(V<v)$. The signal-plus-noise level v can be considered as sample values from probability space with cumulative distribution function G(v). If it is assumed that these samples (target return pulses) are from an identical target distribution and independent, the expected values of Equation F-18 can be taken to obtain the probability of a hit occuring when the target is present:

$$P_{sl}(J,RQT) = \int_0^1 \sum_{K=RQT}^{J} \binom{J}{K} [F(v)]^K [1-F(v)]^{J-K} d[G(v)] \qquad \text{(F-19)}$$

After substituting the appropriate cumulative distribution for signal-plus-noise G(v) and noise F(v), Equation F-19 was used in the analysis to compute the target hit probability. It should be pointed out that the assumption of pulse-to-pulse independence in deriving Equation F-19 implies that the equation will only give estimated values when the target return pulse are correlated in amplitude.

COMPUTER PROGRAM DESCRIPTIONS

Probability of False Alarm Program

This subsection describes a computer program written for the analysis to compute probability of false alarm. The previous sections derived equations for computing the probability of false target hits with and without interference. These false target hits were related to the probability of false alarm from curves generated by the false alarm probability program.

The target detection stage of the (see Figure 4-2) ARTS-IIIA/RDAS maintains a record of the target hits and misses in azimuth for a given range bin. When the consecutive misses in the record equals or exceeds a miss count threshold (3 or 4), the accumulated sum of the target hits in the record is compared with a hit count threshold. If the hit count equals or exceeds the hit count threshold, a target is declared. The record of hits and misses is initialized when the first hit occurs and continues for 30 ACPs. The record is extended beyond the 30th ACP if the hit count threshold at this ACP is satisfied, but the miss count threshold is not.

Because the record azimuth window can vary in length, a mathematical expression describing the hit processing becomes intractable. A straightforward method of calculating the false alarm probability is to employ a Monte Carlo simulation. However, the false alarm probabilities have approximate values of 10^{-6} and would require more than one million repetitions in the simulation to evaluate. Consequently, the computation time on even modern computers would become excessive. For this reason, and to avoid questions of statistical confidence, a deterministic approach was taken to compute the probability of false alarm. A computer program was written which employs a combination of simulation and analytical methods. The technique basically involves identifying all possible combinations of hit and miss sequences which satisfy the target declaration criteria and computing the probability of each occurring. The type of calculations performed by the computer program can be described mathematically by:

$$PFA = \sum_{L=(HCT+MCT)}^{30} \sum_{i=1}^{2^L} f(i) \cdot P_1^{HC_i} (1-P_1)^{MC_i} \qquad \text{(F-20)}$$

where:

PFA = Probability of false alarm

P_1 = Probability of false target hit occurring

HC_i = Hit count (sum of hits) for i th hit/miss sequence combination and record length L

MC_i = Miss count (sum of misses) for i th hit/miss sequence combination and record length L

HCT = Hit count threshold required to be satisfied for target declaration

MCT = Miss count threshold required to be satisfied for target declaration

L= Record length or window width in ACPs

and

$$f(i) = \begin{cases} 1 & \text{target declaration criteria satisfied} \\ 0 & \text{target declaration criteria not satisfied} \end{cases} \qquad \text{(F-21)}$$

The "i" in the above equation signifies a particular hit/miss sequence combination. A computer subroutine algorithm sets f(i) equal to 1 if the particular hit/miss sequence combination satisfies the target declaration criteria and zero otherwise. The upper index of the inner summation indicates that 2^L hit/miss sequence combinations were examined for a given record length (azimuth window) to determine if the target declaration criteria had been met. The probability of each sequence occurring, which satisfies the target declaration criteria, was computed and summed. The outer summation is taken to add the false alarm probabilities for all possible record lengths up to the system maximum (without extension) of 30 ACPs. The lower limit of the summation (HCT + MCT) gives the minimum record length (azimuth window) in which the target declaration criteria can be satisfied. It should be pointed out that Equation F-20 implies that the probability of a noise hit occurring on a given ACP is independent of it occurring on any other ACP. Therefore, the results of the simulation are not applicable to correlated clutter.

The actual implementation of Equation F-20 in the computer program took a slightly different form to save computer time:

$$PFA = \sum_{L=(HCT+MCT)}^{24} \sum_{i=1}^{2^L-2-MCT} f(i) \cdot P_1^{HC_i+2} (1-P_1)^{MC_i+MCT} \qquad \text{(F-22)}$$

This form of the equation reduced the number of binary (hit/miss) sequences that had to be generated and tested for compliance with the target declaration criteria. It takes advantage of the fact that every binary sequence that satisfies the target declaration criteria begins with a hit and ends with a hit plus MCT consecutive misses. For example, with a MCT of 3 the binary sequence takes the form (1.....1000). Therefore only the hit

(1) and miss (0) combinations between the first and last 1 need to be considered. To further save computer time, the program was written to generate false alarm versus record length curves for record lengths up to 24 ACPs. These curves were then used to extrapolate the probability of false alarm for record lengths up to 30 ACPs. The error in the final extrapolated probability of false alarm value due to extrapolation is estimated to be less than 2 percent. This error is small because the contribution to the false alarm probability calculation was relatively small for record lengths greater than 24.

As previously stated, the record of hits and misses are extended by the RDAS beyond 30 ACPs if on the 30th ACP the hit count threshold has been satisfied, but the miss count threshold has not. The contribution of record lengths greater than 30 ACPs to the system probability of false alarm was computed and found to be insignificant.

The sequence of program operations to compute the probability of false alarm is outlined below:

(1) For a given record length (azimuth window), generate all possible hit/miss sequence combinations.

(2) Test each hit/miss sequence combination to determine which satisfy the target declaration criteria.

(3) For each identified hit/miss sequence combination that satisfies the target declaration criteria compute the probability of it occurring using the known probabilities of individual hits or misses occurring.

(4) Add the probabilities computed for each hit/miss sequence combinations occurring that satisfy the target declaration criteria.

(5) Perform the above operations for each record length (azimuth window) up to 24 ACPs.

(6) Generate a curve of false alarm probability versus record length.

Probability of Target Detection Program

This subsection describes a computer program that was written to compute probability of target detection. The program generated curves that were used in the analysis to relate probability of target hit to probability of target detection.

Basically, the computer program uses the Monte Carlo technique to simulate target hit and miss sequences and then counts the number of hit/miss sequence cases which satisfy the target declaration criteria. The percentage of hit/miss sequence cases that satisfy the target detection criteria was

computed to obtain the predicted target detection probability. A total of 30 ACPs were considered in each simulated sequence of hits and misses. The first five and last five ACPs of the sequence considered only the presence of noise in the range bin while the middle 20 ACPs in the sequence considered the target to be present. It was assumed in the simulation that the target was present for 20 ACPs because this is the typical number of return pulses received by an ASR-7 or ASR-8 radar from an aircraft target. This is evident from evaluation of Equation 3-21 for typical ASR-7 and ASR-8 radar parameter combinations. Noise only ACPs, before and after the target, were included in the simulation because noise in these range bins affect the probability of the target being detected. In particular, the noise in the range bins (ACPs) before the target increases the probability of the hit count threshold being satisfied, and noise in the range bin following the end of the target decrease the probability of the miss count threshold being satisfied. A number of test simulations were conducted to determine how many range bins should be included before and after the target range bins. The test simulations indicated that including five noise only range bins before and after the target range bins provides a good trade-off between computer time and predicted detection probability accuracy. It is estimated that including only five range bins before and after the target range bins, instead of an infinite number, introduces less than 1 percent error in the predicted target detection probability.

The Monte Carlo simulation of the hit/miss sequence is described mathematically by the function:

$$f_j(U) = \begin{cases} 1 & \text{for } U \leq P_1 \\ 0 & \text{for } U > P_1 \end{cases} \qquad \text{(F-23)}$$

where:

j = The particular ACP index number which can range from 1 to 30,

U = Random number uniformly distributed between 0 and 1.0

P_1 = The probabillity of a hit (logical 1) occurring.

The value of P_1 in Equation F-22 depends on the particular ACP and if noise only or signal-plus-noise is considered present in the range bin corresponding to a particular ACP. The value of P_1 for the first five and last five ACPs (j = 1-5 and 26-30) in each simulated hit/miss sequence corresponds to the probability of a target hit occurring due to only noise and was computed from Equation 4-5. A noise hit probability of 0.08 was used for a rank quantizer threshold setting of 23, and a noise hit probability of 0.04 for a rank quantizer threshold of 24. The value of P_1 in Equation F-23

for the middle 20 ACPs (j = 6-25) in each simulated hit/miss sequence represents the probability of a hit occurring due to the presence of an aircraft target. The simulation considered the probability of a hit occurring on a given ACP to be independent of the probability of it occurring on any other ACP. In other words, the simulation does not consider the possibility of pulse-to-pulse correlation of the target or clutter return pulses. In addition, the computed detection probabilities are for one antenna rotation and do not include the improved detection characteristics that can result from antenna scan-to-scan target tracking.

As stated previously, the program was used to generate target detection probability versus target hit probability curves (see Figures 4-27, 4-28 and 4-29). Each curve corresponds to a particular combination of detection parameter settings (rank quantizer threshold, hit count threshold, and miss count threshold). Each point on the curve was determined from ten thousand repeated hit/miss sequence simulations. Other points on the curves were obtained by performing these simulations with different target hit probability P_1 values substituted in Equation F-23. However, the value of P_1 in Equation F-23 for noise only ACPs was held constant for all points on a given curve.

It should be pointed out that the simulations did not include the effect of interference on the noise hit probabilities corresponding to the range bins not occupied by the target. This drastically reduced the number of curves and computer time required for the target detection calculations. Neglecting the interference effects on noise hit probabilities did not significantly affect the computed detection probability values. This fact is evident from the detection probability curves in Figures 4-27 and 4-28. The curves in Figure 4-27 are for a rank quantizer threshold of 23 or equivalently (see Equation 4-5) a noise hit probability of 0.04, and the curves in Figure 4-28 for a noise hit probability of 0.08. Comparison of corresponding curves in Figures 4-27 and 4-28 for the same hit and miss count thresholds indicates a 0.04 change in noise hit probability does not change the predicted detection probability by more than 0.02. It was shown in the false alarm portion of the analysis (see TABLES 4-3 and 4-5) that continual interference from three radars does not change the noise hit probability by more than 0.006. This indicates that the effect of interference on noise hit probability is small enough to be neglected in the detection probability calculation.